ISSN: ISSN: 0974-5823 Vol. 7 No. 2 February, 2022

International Journal of Mechanical Engineering

Polymer composites with 97% UV-blocking and high pathogenic bacteria inhibition using PVA/PVP polymer blend encapsulated with Sb_2O_3NPs: morphological and optical features

Alhak A. M. Hassan[1], Karar Abdali[2], Khalid Haneen Abass[3], Ehssan Al-Bermany[3], Fouad Sh. Hashim[3], Abdulazeez O[1].

[1]Physics Department, College of Science, University of Babylon, Iraq

[2] Ministry of Education, Baghdad, Iraq

[3] Physics Department, College of Education for Pure Sciences, University of Babylon, Iraq

Abstract

The application and development of natural antibacterial (ANB) nanocomposites (NCs) films have always been the concern of biomedical studies. In the current study, three different amounts of antimony trioxide nanoparticles (Sb_2O_3NPs) were incorporated with (60:40)wt.% of polyvinyl alcohol (PVA) and poly(N-vinyl pyrrolidone) (PVP) polymer matrix (PM) via casting method. The samples were labeled as N1, N2, and N3 depending on the PM to Sb_2O_3NPs ratio. The NCs films were investigated by light microscope (LM), Fourier transformation infrared (FTIR) and UV/visible spectrum. The NPs were perfectly diffused on the homogeneous surface of PM without aggregations. The sharpness of FTIR peaks increased with the increasing of Sb_2O_3NPs. The UV/visible properties were measured with wavelength between 190 to 1100 nm. The optical coefficients improved after loading except the transmittance (T%) and indirect energy gap (E_g). The nanocomposite (NC) films absorbed about 97% from the UV ray in the λ=220 nm. The absorption edges decreased with the increase of energy from 4.0 eV to 3.85 eV. The indirect E_g values decreased from 4.0 eV to 3.8 eV. Each type of gram negative pathogenic bacteria was affected by the addition of Sb_2O_3NPs. The inhibition zones were increased with the increasing of NPs contents from (0-9.5) mm for E-coli and from (0-14.4) mm for Proteus mirabilis bacteria.

Keywords: PVP, Sb_2O_3, Pathogenic bacteria, Optical properties.

1. Introduction

Nanomaterials and nanotechnology are of much interest for the development of new ANB approaches, based on either novel biomaterials or on enhancing the biological features of the existing ones [1]. Currently, in a sustainable and eco-friendly driven approach, many studies are directed to design both clinically and environmentally safe nanomaterials for ANB applications. Hybrid polymer NCs are a novel type of material with unique physical and chemical properties. These NCs have recently attracted serious research attention due to their tangible potential for a wide range of applications in environmental solutions and the resolution of many environmental aspects [1]. The dynamic interface between NPs and polymer basis is the most challenging aspect of NCs [2]. Hybrid polymer NCs bring a novelty of several type of materials with unique physical and chemical properties [1,2]. These NPs have nano dimensions, large specific area and energy sites in the surfaces are formed that underline the importance of polymer-nanoparticles interactions. The physical properties of NCs change and improve could be achieved with using these nano materials, Therefore, imperative to study the incorporation process between nanoparticles and polymer based [1,3]. Polyvinyl alcohol (PVA) is a water-soluble polymer (WSP) with a chemical structure of CH_3CHOH $(CH_2\text{-}CHOH)_n$. It is derived from vinyl acetate [4]. It has various grades of viscosity [4,5]. PVA is well known for its use in the manufacture of fabrics, including wide and several applications [6,7]. PVP has a number of vinyl polymers with stable at different temperatures, hygroscopic and water soluble polymer [8-10]. In conjunction with halogenated materials, the main use of Sb_2O_3 is as a flame retardant synergist [11]. For polymers to have a retardant of flame action, the halides combination and antimony is critical, as it aids in the shaping of less flammable chars [11,36-48]. The optical properties of nanoparticles of Sb_2O_3 are strongly conditioned on the diameters of the nanoparticle. The smaller diameter of Sb_2O_3 almost absorbs light and has peaks around 400 nm, whereas the larger domain has increase dispersion and peaks that extend and transfer to longer wavelengths of red-shifting. Sb_2O_3 is a cheap and commercial raw nano partial that is considered a good semiconducting material [12]. The main aim of this research is to study the effect of adding Sb_2O_3NPs on morphological, optical properties, and pathogenic bacteria of PVA/PVP polymer blend.

2. Experimental study

2.1 Materials

PVA (18000 Mw and 99.9% of purity) was equipped by (DIDACTIC), PVP (40000 Mw and 99.9% of purity) was supplied by (Central Drug House, CDH) and Sb_2O_3NPs was purchased from (Sigma Aldrich Co.) with (20-30) nm average grain size and (99.5%) purity.

2.2 Synthesis of NCs

The (60:40) wt.% of PVA and PVP was separately dissolved in (50 mL) distilled water as an MB. The mixture was thereafter stirred for 3 hrs. Using a magnetic stirrer for 45 °C. The MB solution was cast and left to dry for a week via Petri dish by casting method. In the doping process 0, 0.02 and 0.04 Sb_2O_3NPs wt.% were added to the MB solution in steps of 40 mL, as shown in Table 1. To homogenize these NCs, stirring was made for 30 min. The thicknesses of NCs films were calculated to be between 0.070 and 0.080 cm.

Table 1. The purification methods of N1, N2 and N3 samples.

Sample ID	Ratio of wt.%			Total Mixing Time h	Drying Method
	PVA	PVP	Sb_2O_3NPs		
N1	0.600	0.400	0.00	3	Freeze drier 50 ± 5 C° under air
N2	0.588	0.392	0.02	4	
N3	0.576	0.384	0.04	4	

2.3 Characterizations

The LM images were investigated via Nikon: Olympus model. The samples were chemically characterized in the wavenumber range between (4000–400) cm^{-1} using (Vertex 701, Bruker FTIR). A double-beam spectrophotometer (UV/1800) was used to study the UV/Visible properties. The ANB properties were computed using the disk diffusion method.

3. Results and discussions

3.1 The LM images

Figure 1. represents the optical microscopy images of PVA/PVP blends without and with Sb_2O_3NPs contents at (100X) magnification power. Figure (1-A) shows that the polymer blend was correctly and uniformly dissolved in the solvent. The diffusion of Sb_2O_3NPs in the blend was represented in the (B and C) parts of the same Figure. Part (C) explains the nature of physical interaction between Sb_2O_3NPs and PM due to the high ratio of NPs content. In these photomicrographs, the nature of surface of PVA/PVP blend were enhanced after loading. It may be due to the NPs proper association with the matrix. Sb_2O_3NPs contributed to changes in the composition of the surface, and uniformly distributed. The growth mechanism was enhanced after incorporations, this is because the Sb_2O_3NPs were good diffused in the PM [13].

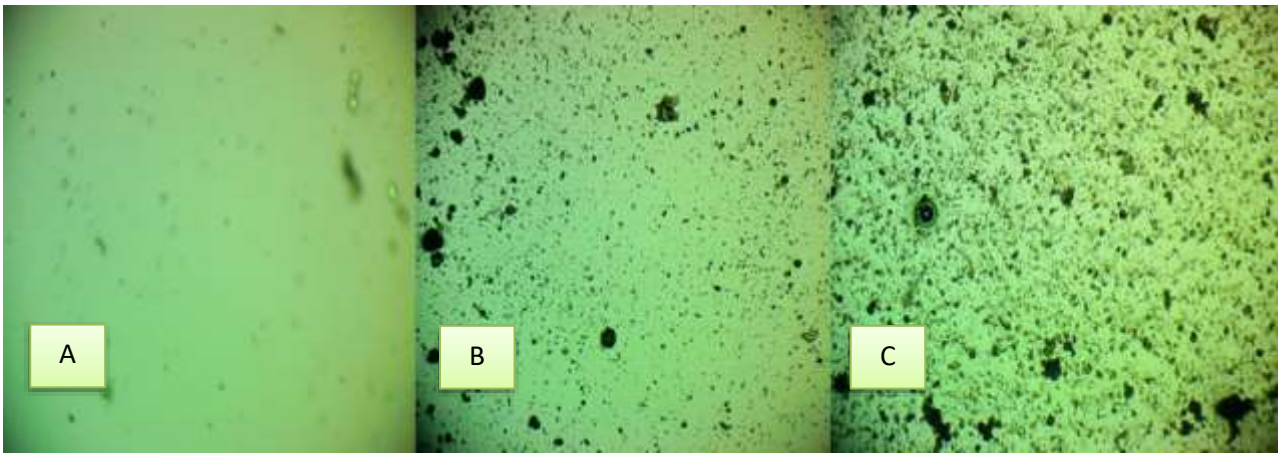

Figure 1. Photomicrographs (100X) of A) N1, B) N2, C) N3 samples.

3.2 The chemical properties

The chemical properties of N1, N2 and N3 samples were experimentally investigated by FTIR spectrums as shown in Figure 2. The FTIR spectrums were calculated in the optical range between (500-4000) cm^{-1}. The spectrums also refer to the excellent compatibility of PVA and PVP when blended together with each other. The OH groups and the (C=O) groups shaped miscible mixes via H bonding [13]. This creates a strong incentive for NPs to be incorporated into the PVA/PVP blend's foundation [14,15]. There is many physical interactions happened between the matrix polymer blend and Sb_2O_3NPs. The intensity of FTIR peaks increased after incorporation.

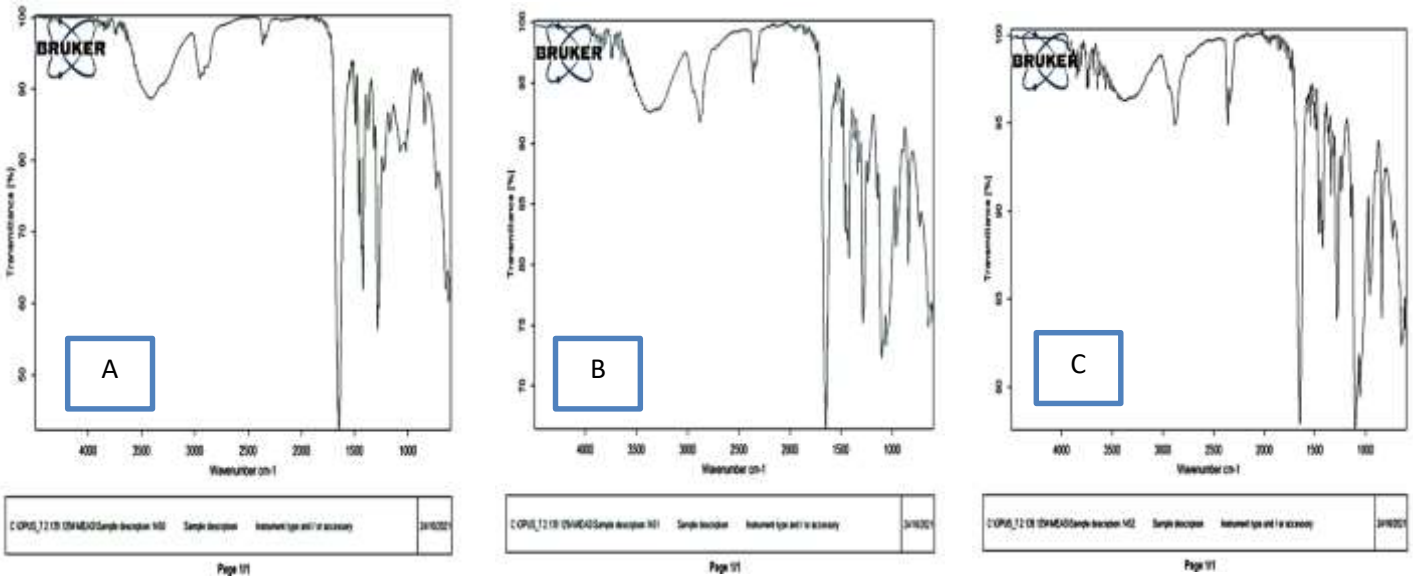

Figure 2. FTIR spectrum of A) N1, B) N2, C) N3 samples.

3.3 The UV/Visible properties

The UV/Visible properties of PVA/PVP PM and its additives with (0.02 and 0.04)wt.% Sb_2O_3NPs in the λ between (190 to 1100) nm were investigated. The absorption spectrums of PM and NCs films were presented in the Figure 3. The NCs films were absorbed about 97% from UV ray in the (λ=220) nm. In the visible and near IR region, this absorbance spectrum of prepared films has low values, since the incident photons do not have enough energy to interact and thus transmit with atoms at high wavelengths. The interaction between the incident photon and the films will occur when the wavelength decreases, thus increasing the absorbance [16]. Furthermore, the addition of Sb_2O_3NPs to the blend clearly improved the optical absorption spectrum and this is linked to the best diffusion and homogeneity of NPs in the films, suggesting an effect of the amount of NPs on the polymer feature [17].

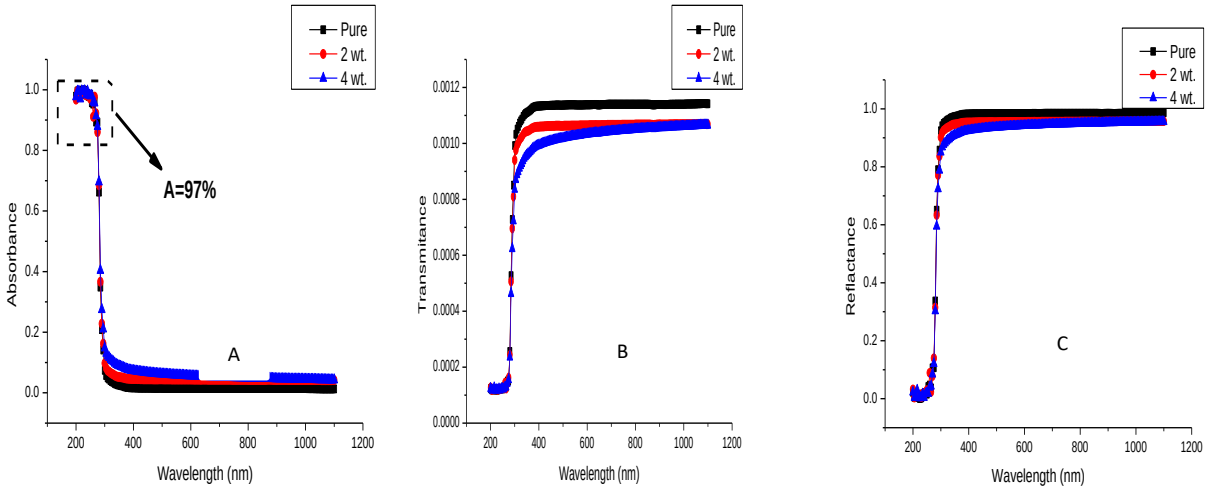

Figure 3. A) Absorbance vs. wavelength, B) Transmittance vs. wavelength, C) Reflectance vs. wavelength.

As shown in the Figure (3C), the reflectance spectrum of pure PVA/PVP and its additives was also studied as a function of wavelength. It states that the reflectance of NCs films was directly proportional with the percentage weight of the Sb_2O_3NPs, but inversely proportional to the wavelength. Therefore, this activity has a high reflectance in the UV region due to the increasing of NCs density. The refractive index (RI) has the same reflectance behavior Figure 4 since, as in equation (1), below depends on R. [18].

$$n = [(1 + \sqrt{R})/(1 - \sqrt{R})] \quad \ldots\ldots\ldots\ldots\ldots\ldots (1)$$

The absorption coefficient (α) decreased as the wavelength of prepared films increased, because it relied on absorbance. The (α) of the NCs were determined by [19]:

$$\alpha = 2.303\ A/t \quad \text{……..……...…….(2)}$$

The NCs extinction coefficient (k) has been calculated by [19]:

$$k=(\alpha\lambda)/4\pi \quad \text{……...(3)}$$

In general, k values increased with the increasing of Sb_2O_3NPs for prepared films. Figure 4 shows that the relationship between n or k values and the wavelength for MP and NCs films . It can be observed that with the increasing of Sb_2O_3NPs and energy (hf), the absorption coefficient increase as shown in Figure 5. These values are lower than (10^4 cm^{-1}), which allows the likelihood of indirect transitions to increase.

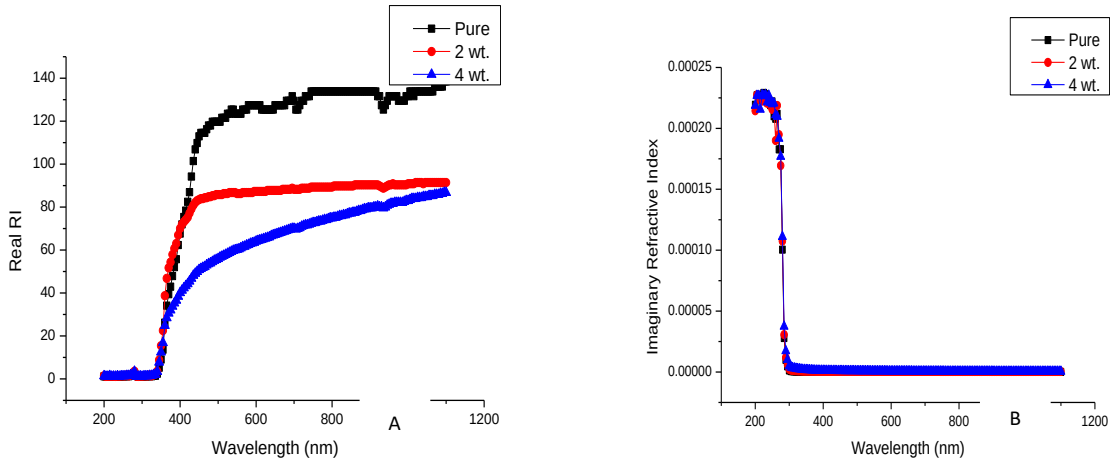

Figure 4. The refractive index vs. wavelength of (PVA/PVP)/Sb_2O_3 NCs, A) Real part, B) Imaginary part.

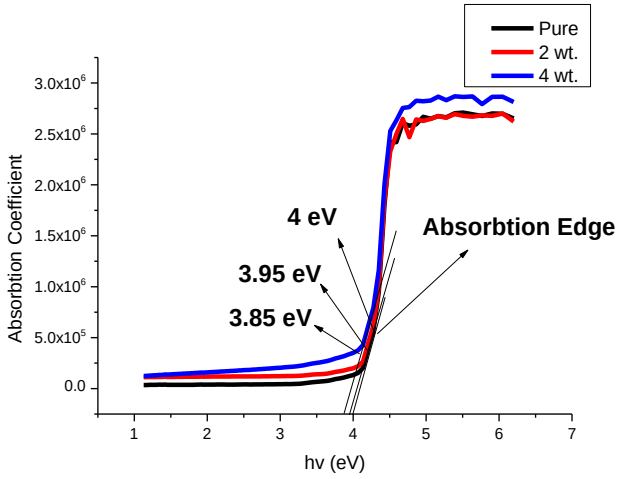

Figure 5. The absorption coefficient vs. wavelength of (PVA/PVP)/Sb_2O_3 NCs.

The optical energy gaps of (PVA-PVP)/Sb_2O_3NPs films were calculated using the Tauc model [19]:

$$\alpha\ h\upsilon \approx B(h\upsilon - E_g)^n \quad \text{…….. (4)}$$

(n) is a transformation parameter and (B) is constant. The plot of $(\alpha h\nu)^{1/2}$ with energy refers to the indirect electron transformations. The straight line of photon energy extrapolation at zero $(\alpha h\nu)^{1/2}$ represents E_g as shown in Figure 6. The increasing of Sb_2O_3NPs leads to decreasing the energy gap values. These NCs films are semiconductors. Such observations were shown in the Table 2.

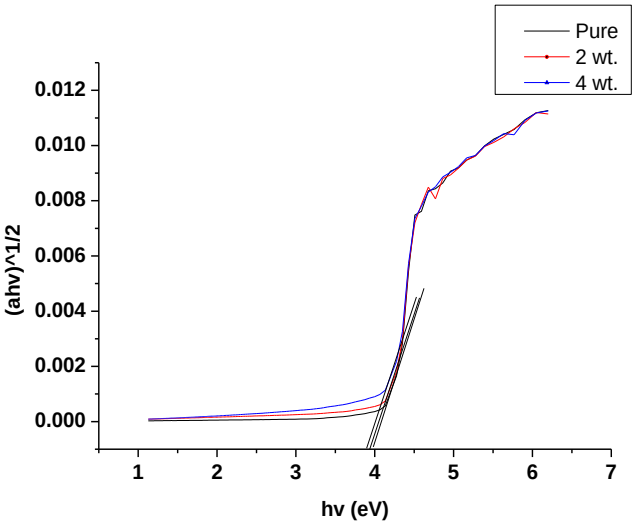

Figure 6. A plots of $(\alpha h\nu)^{1/2}$ vs. photon energy of (PVA/PVP)/Sb_2O_3 NCs.

Table 2. Optical energy gap of N1, N2 and N3 samples.

Sample ID	Optical energy gap (eV)
N1	4.00
N2	3.90
N3	3.80

3.4 Anti- pathogenic bacteria application

In present study the NCs antibacterial properties were investigated using the disk diffusion method. The Nutrient agar plates were used as a culture media for pathogenic bacterial growth. Sterilized paper dishes containing NCs were putted in each plate. The pathogenic bacteria was growing up in the Petri dish at (45°C) for (25 hrs.). The clear zones uniform width across each disk in all directions demonstrates that the NPs diffuse uniformly in the polymer matrix. Calculating the diameter of disk in addition of the surrounding area is the typical method for measuring the inhibition regions [1]. The co-culture method was used for calculating the ANT effect of NCs. The bacterial culture of two pathogenic bacteria was grown in nutritious medium with NCs at the ratio of 0.5/0.5 (vol./vol.). The nutrient broth was used as a control medium. After the incubation 0.5 mL of each cultures were diluted for each one respectively. The 0.05 mL of dilution specimens was taken and spread on agar plates. The plates were incubated at 45 °C for 25 h. The colonies were calculated and the effects of inhibition were assessed and computed the reducing of bacterial growth by [20]:

$$R = ((A-B)/A) \times 100\% \quad \ldots\ldots\ldots\ldots\ldots\ldots (5)$$

where R is the reducing factor of bacterial growth, A is the no. of controls bacterial colonies, B is the no. of treatments bacterial colonies. Table 3. Shows that the effects of the inhibition zones formed in the vicinity disks, which were counted and tallied. With the addition of Sb_2O_3NPs, the inhibition zone and bactericidal properties increased, as shown in Figures 7 and 8. The Proteus mirabilis pathogenic bacteria was found to be more resistant to (PVA/PVP)-Sb_2O_3 NCs film than E. coli bacteria. Many researchers were studied the effect of NPs, metal and metal oxide on the inhibition of various pathogenic bacteria as reported in [21-30]. The variations in cell structure, morphology, metabolism and degree of contact of organisms with NPs could explain the variance in resistance of gram negative bacteria diffusions. For example, gram-negative Proteus mirabilis has a higher amine abundance and carboxyl groups on its cell surface, as well as a higher affinity of copper for these groups. Proteus mirabilis has higher responded to Sb_2O_3NPs [29,30]. The study of ANB efficiency of this NCs films is a comparative study with [24,31-35]. The previous studies and the current study concluded that the PVA/PVP polymer blend don't effects on any pathogenic type of bacteria. As reported in these studies the adding of NPs enhanced the ability of this polymer blend to inhibits the various type of pathogenic bacteria. The cause for the ANB efficiency of NCs may be because the existence of species of reactive oxygen (ROS) created by various NPs. The chemical reaction between hydrogen peroxide and the proteins of membrane or between the chemical generated in the existence of NCs and the outer bilayer of bacteria could be the cause for the ANB efficiency of NCs. The hydrogen peroxide created enters the bacteria cell membrane and inhibits them. The NCs continue to be in reaction with defunct bacteria once the peroxide of hydrogen is created. Therefore, foiling moreover bacterial influence and continue to product and emission the peroxide of hydrogen to the

medium. The reasonable mechanism action is which the NPs in NCs are creating the (–ve) charges that produce the electromagnetic attraction between the NPs and the microbes. The microbes get oxidized and die instantly after the attraction. The major mechanism which reasoned the ANB of NCs via the NPs might be through stress of oxidative reasoned by ROS. The ROS involves radicals such as (O^{-2}), (–OH), (H_2O_2) and ($^1O_2$) could be the cause damaging the DNA and proteins in the bacteria. ROS could have been created via the current metal oxide leaded to the inhibition of most bacteria.

Table 3. The average inhibition zones of N1, N2 and N3 samples.

Sample ID	Inhibition Zone (mm)	
	E. coli	Proteus mirabilis
N1	0	0
N2	8.1	8.8
N3	9.5	14.4

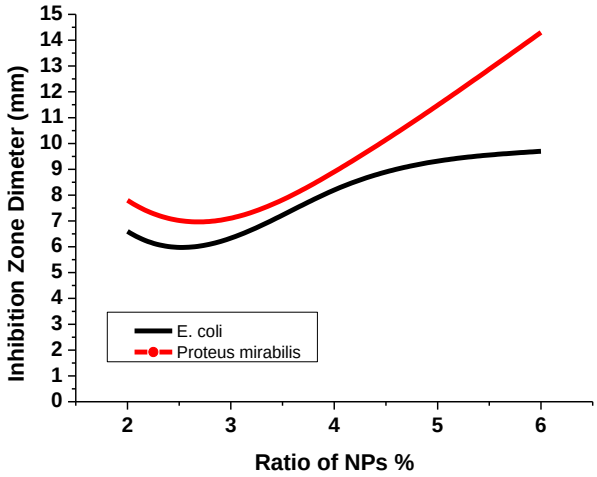

Figure 7. The average of inhibition zones of (PVA/PVP)/NCs vs. the ratio of NPs.

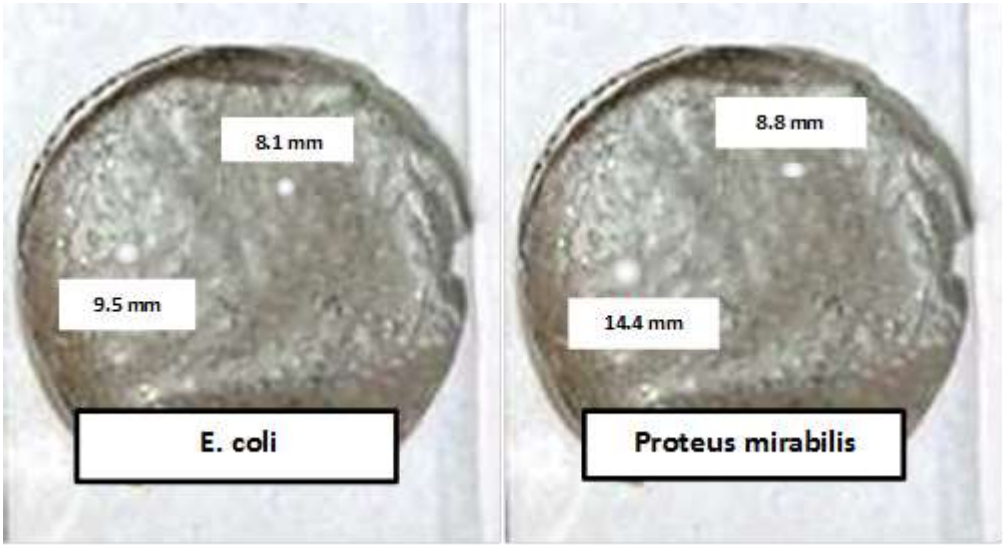

Figure 8. ANB efficiency of the NCs films against E. coli and Proteus mirabilis bacteria.

4. Conclusion

The PM and NCs films were successfully prepared by the dry casting method. The LM images show that the materials were correctly and uniformly dissolved in the solvent, the Sb_2O_3NPs good diffused in the PM and the growth mechanism enhanced after incorporations. The FTIR spectrum refers to the excellent compatibility of PVA, PVP and NPs when mixing together with each other. The NCs films blocked about 97% from the UV ray in the λ=220 nm. The absorption coefficients decreased with the increase of energy from 4.0 eV to 3.85 eV. The indirect Eg values decreased from 4.0 eV to 3.8 eV. The Sb_2O_3NPs clearly affect gram-

negative pathogenic bacteria. The inhibition zones increased with the increasing of Sb_2O_3NPs contents from (0-8.2) mm for E-coli and from (0-8.9) mm for Proteus mirabilis bacteria.

References

[1] Kadhim, M. A., & Al-Bermany, E. (2021). New fabricated PMMA-PVA/graphene oxide nanocomposites: Structure, optical properties and application. Journal of Composite Materials, 55(20), 2793-2806.

[2] Yetisgin A, Cetinel S, Zuvin M, Kosar A., Kutlu O (2020) Therapeutic nanoparticles and their targeted delivery applications. Molecules. 25: 2193.

[3] M.Vadive, S. Sultan, A. Bahadur, Sh. Athimoolam (2020) Structural elucidation, hydrogen bonding motifs and solid state properties of p-toluenesulfonate salt of β-alaninine for optoelectronic device application. J. Mol. Structure. 1221: 128820.

[4] Aldulaimi, N.R. and Al-Bermany, E., 2021, August. New Fabricated UHMWPEO-PVA Hybrid Nanocomposites Reinforced by GO Nanosheets: Structure and DC Electrical Behaviour. In Journal of Physics: Conference Series (Vol. 1973, No. 1, p. 012164). IOP Publishing.

[5] J. Zeng, C. Peng, R. Wang, Y. Liu, X. Wang, J. Liu (2019) Large-scale synthesis of hierarchical SnO spheres assisted with poly (N-isopropylacrylamide) for high lithium storage capacity. Ceram. Int. 45: 1246-1250.

[6] J. E. Mark (1999) Polymer Data Handbook. New York: Oxford university.2nd.ed. ISBN: 9780195181012.

[7] Al-shammari, A.K. and Al-Bermany, E., 2021, August. New Fabricated (PAA-PVA/GO) and (PAAm-PVA/GO) Nanocomposites: Functional Groups and Graphene Nanosheets effect on the Morphology and Mechanical Properties. In Journal of Physics: Conference Series (Vol. 1973, No. 1, p. 012165). IOP Publishing.

[8] Karar Abdali (2022) Structural, Morphological, and Gamma Ray Shielding (GRS) Characterization of HVCMC/PVP/PEG Polymer Blend Encapsulated with Silicon Dioxide Nanoparticles. Silicon. 14(1): 6-10. https://doi.org/10.1007/s12633-022-01678-8.

[9] A. Jenkins (2013) Polymer Science: A material Science Handbook. North Holland Publishing. Kindle ed. ASIN: B01DY7XF70.

[10] M. Teodorescu and M. Bercea (2015) Poly(vinylpyrrolidone) – A Versatile Polymer for Biomedical and Beyond Medical Applications. Polymer-Plastics Technology and Engineering. 54(9): 923-943.

[11] Z. Cheng, T. Milne, P. Salter, j. Kim, S. Humphrey, M. Booth, H. Bhaskaran (2021) Antimony thin films demonstrate programmable optical nonlinearity. Science Advances. 10:1126.

[12] T. Cebriano, B. Me´ndez, J. Piqueras (2013) Sb_2O_3 microrods: self-assembly phenomena, luminescence and phase transition. J Nanoparticle Res. 15: 1667.

[13] Al-Khalaf A., Karar Abdali, Mousa A., Zghair M (2019) Preparation and structural properties of liquid crystalline materials and its transition metals complexes. Asian Journal of Chemistry. 31(2): 393-395.

[14] Y. Guo, X. Zuo, Y. Xue, J. Tang, M. Gouzman, Y. Fang, Y. Zhou, L. Wang, Y. Yu, M. Raf (2020) Engineering thermally and electrically conductive biodegradable polymer nanocomposites. Compos. B Eng. 189: 107905.

[15] H. Hu, F. Zhang, S. Luo, W. Chang, J. Yue, C. Wang (2020) Recent advances in rational design of polymer nanocomposite dielectrics for energy storage. Nano Energy. 74: 104844.

[16] Karar Abdali, Lamis F., Alhak A., Abdulazeez O., Ali A (2018) Enhancing Some Physical Properties of Cosmetic Face Powders. Journal of Global Pharma Technology. 10(3): 75-78.

[17] Abdulazeez O. Ali J., Ali S., Karar Abdali, Shirren R (2017) Synthesis of Hyperbranched Polymers and Study of its Optical Properties. Journal of Engineering and Applied Sciences. 12(6): 7800-7804.

[18] B. Max and W. Emil (1999) Principles of Optics",7th expanded ed., CUP Archive. p. 22. ISBN 978-0-521-78449-8.

[19] J. Carter (2019) Cosmic Creation and Evolution of Matter and Energy. 2nd ed. lulu.com. ISBN-10: 0359721001.

[20] Ghosh S., Upadhay A., Singh A., Kumar A (2010) Investigation of antimicrobial activity of silver nano particle loaded cotton fabrics which may promote wound healing. International Journal of Pharma and Bio Sciences. 1(3): 1-10.

[21] R. Mohammed, M. Habeeb, A. Hashim (2020) Effect of Antimony Oxide Nanoparticles on Structural, Optical and AC Electrical Properties of (PEO-PVA) Blend for Antibacterial Applications. International Journal of Emerging Trends in Engineering Research. 8(8): 4726-4738.

[22] A. Azam, A. Ahmed, M. Oves, M. Khan, S. Habib, A. Memic (2012) Antimicrobial activity of metal oxide nanoparticles against gram-positive and gram-negative bacteria: a comparative study. Int. J. Nanomedicine. 7: 6003.

[23] A. Azzam, M. Hazaa, A. El Saeed, M. Hamed (2016) Antibacterial activity of cupric oxide nanoparticles against pathogenic bacteria. J. Basic Environ. Sci. 3:90-93.

[24] S. Mallakpour and S. Mansourzadeh (2018) Sonochemical synthesis of PVA/PVP blend nanocomposite containing modified CuO nanoparticles with vitamin B_1 and their antibacterial activity against Staphylococcus aureus and Escherichia coli. Ultrasonics Sonochemistry J. 43: 91-100.

[25] Mohamed E., Sultan A., Mohsen M., Mohamed I., Mohamed H (2022) Fabrication of Nanofibers Based on Hydroxypropyl Starch/Polyurethane Loaded with the Biosynthesized Silver Nanoparticles for the Treatment of Pathogenic Microbes in Wounds. Polymers. 14(2): 318.

[26] Lúcia F., Cláudia M., Martijn R., Isabel C (2022) Antimicrobial Food Packaging Based on Prodigiosin-Incorporated Double-Layered Bacterial Cellulose and Chitosan Composites. Polymers. 14(2): 315.

[27] W. Chen, P. Zhu, Y. Chen, Y. Liu, L. Du, C. Wu (2022) Iodine Immobilized UiO-66-NH2 Metal-Organic Framework as an Effective Antibacterial Additive for Poly (ε-caprolactone). Polymers. 14(2): 283.

[28] J. Jeong, Y. Kim, Y. Hu, S. Jung (2022) Bacterial Succinoglycans: Structure, Physical Properties and Applications. Polymers. 14(2): 276.

[29] Q. Cheng, A. Benozir, Y. Liu, Y. Peng, D. Diaz, Z. Shi, Z. Cui, R. Narain (2022) Antifouling and Antibacterial Polymer-Coated Surfaces Based on the Combined Effect of Zwitterions and the Natural Borneol. ACS Appl. Mater. Interfaces. 13(7): 9006–9014.

[30] P. Badica, N. Batalu, M. Burdusel, M. Grigoroscuta, G. Aldica, M. Enculescu, G. Gradisteanu, M. Popa, L. Marutescu, B. Dumitriu, L. Olariu, A. Bicu, B. Purcareanu, L. Operti, V. Bonino, A. Agostino, M. Truccato, M. Chifiriuc (2021) Antibacterial composite coatings of MgB2 powders embedded in PVP matrix. Scientific reports. 11(1): 9591.

[31] H. Yu, X. Xiaoyi, X. Chen, T. Lu (2007) Preparation and antibacterial effects of PVA-PVP hydrogels containing silver nanoparticles. Journal of Applied Polymer Science. 103(1): 125-133.

[32] Jehan A., Zainab A., Hamsa A (2016) Antibacterial effect and structural properties of PVA-PVP-Ag nanocomposites. Ejbps. 3: 35-41.

[33] Y. Nho, Y. Lim, H. Gwon, E. Choi (2009) Preparation and characterization of PVA/PVP/glycerin/antibacterial agent hydrogels using γ-irradiation followed by freeze-thawing. Korean J. Chem. Eng. 26(6): 1675-1678.

[34] M. Abd El-Kader, M. Elabbasy, A. Adeboye, A. Menazea (2021) Nanocomposite of PVA/PVP blend incorporated by copper oxide nanoparticles via nanosecond laser ablation for antibacterial activity enhancement. Polymer Bulletin. 5: 3975.

[35] E. Doğan, P. Tokcan, M. Diken, B. Yilmaz, B. Kizilduman, P. Sabaz (2019) Synthesis, Characterization and Some Biological Properties of PVA/PVP/PN Hydrogel Nanocomposites: Antibacterial and Biocompatibility. Advances in materials science. 19: 32-45.

[36] Vakili-Samiani, S., Jalil, A. T., Abdelbasset, W. K., Yumashev, A. V., Karpisheh, V., Jalali, P., ... & Jadidi-Niaragh, F. (2021). Targeting Wee1 kinase as a therapeutic approach in Hematological Malignancies. *DNA repair*, 103203. https://doi.org/10.1016/j.dnarep.2021.103203

[37] NGAFWAN, N., RASYID, H., ABOOD, E. S., ABDELBASSET, W. K., Al-SHAWI, S. G., BOKOV, D., & JALIL, A. T. (2021). Study on novel fluorescent carbon nanomaterials in food analysis. *Food Science and Technology*. https://doi.org/10.1590/fst.37821

[38] Marofi, F., Abdul-Rasheed, O. F., Rahman, H. S., Budi, H. S., Jalil, A. T., Yumashev, A. V., ... & Jarahian, M. (2021). CAR-NK cell in cancer immunotherapy; A promising frontier. *Cancer Science*, *112*(9), 3427. https://doi.org/10.1111/cas.14993

[39] Abosaooda, M., Wajdy, J. M., Hussein, E. A., Jalil, A. T., Kadhim, M. M., Abdullah, M. M., ... & Almashhadani, H. A. (2021). Role of vitamin C in the protection of the gum and implants in the human body: theoretical and experimental studies. *International Journal of Corrosion and Scale Inhibition*, *10*(3), 1213-1229. https://dx.doi.org/10.17675/2305-6894-2021-10-3-22

[40] Jumintono, J., Alkubaisy, S., Yánez Silva, D., Singh, K., Turki Jalil, A., Mutia Syarifah, S., ... & Derkho, M. (2021). Effect of Cystamine on Sperm and Antioxidant Parameters of Ram Semen Stored at 4° C for 50 Hours. *Archives of Razi Institute*, *76*(4), 923-931. https://dx.doi.org/10.22092/ari.2021.355901.1735

[41] Raya, I., Chupradit, S., Kadhim, M. M., Mahmoud, M. Z., Jalil, A. T., Surendar, A., ... & Bochvar, A. N. (2021). Role of Compositional Changes on Thermal, Magnetic and Mechanical Properties of Fe-PC-Based Amorphous Alloys. *Chinese Physics B*. https://doi.org/10.1088/1674-1056/ac3655

[42] Chupradit, S., Jalil, A. T., Enina, Y., Neganov, D. A., Alhassan, M. S., Aravindhan, S., & Davarpanah, A. (2021). Use of Organic and Copper-Based Nanoparticles on the Turbulator Installment in a Shell Tube Heat Exchanger: A CFD-Based Simulation Approach by Using Nanofluids. *Journal of Nanomaterials*. https://doi.org/10.1155/2021/3250058

[43] Mohaddeseh Rahbaran, Ehsan Razeghian, Marwah Suliman Maashi, Abduladheem Turki Jalil, Gunawan Widjaja, Lakshmi Thangavelu, Mariya Yurievna Kuznetsova, Pourya Nasirmoghadas, Farid Heidari, Faroogh Marofi, Mostafa Jarahian, "Cloning and Embryo Splitting in Mammalians: Brief History, Methods, and Achievements", *Stem Cells International*, vol. 2021, Article ID 2347506, 11 pages, 2021. https://doi.org/10.1155/2021/2347506

[44] Jalil, A.T.; Ashfaq, S.; Bokov, D.O.; Alanazi, A.M.; Hachem, K.; Suksatan, W.; Sillanpää, M. High-Sensitivity Biosensor Based on Glass Resonance PhC Cavities for Detection of Blood Component and Glucose Concentration in Human Urine. *Coatings* **2021**, *11*, 1555. https://doi.org/10.3390/coatings11121555

[45] Chupradit, S.; Ashfaq, S.; Bokov, D.; Suksatan, W.; Jalil, A.T.; Alanazi, A.M.; Sillanpaa, M. Ultra-Sensitive Biosensor with Simultaneous Detection (of Cancer and Diabetes) and Analysis of Deformation Effects on Dielectric Rods in Optical Microstructure. *Coatings* **2021**, *11*, 1564. https://doi.org/10.3390/coatings11121564

[46] Bokov, D., Turki Jalil, A., Chupradit, S., Suksatan, W., Javed Ansari, M., Shewael, I. H., ... & Kianfar, E. (2021). Nanomaterial by Sol-Gel Method: Synthesis and Application. *Advances in Materials Science and Engineering*, *2021*. https://doi.org/10.1155/2021/5102014

[47] Shabgah, A. G., Al-Obaidi, Z. M. J., Rahman, H. S., Abdelbasset, W. K., Suksatan, W., Bokov, D. O., ... & Navashenaq, J. G. (2022). Does CCL19 act as a double-edged sword in cancer development?. *Clinical and Experimental Immunology*, *20*, 1-12. , https://doi.org/10.1093/cei/uxab039

[48] Kartika, R., Alsultany, F. H., Jalil, A. T., Mahmoud, M. Z., Fenjan, M. N., & Rajabzadeh, H. (2021). Ca12O12 nanocluster as highly sensitive material for the detection of hazardous mustard gas: Density-functional theory. *Inorganic Chemistry Communications*,109174. https://doi.org/10.1016/j.inoche.2021.109174